

Accounting for Backwater Effects in Flow Routing by the Discrete Linear Cascade Model

Jozsef Szilagyi¹ and Pal Laurinyecz²

Abstract: Flow-routing at a tributary (Koros River) of the Tisza River in Hungary was achieved by relating the storage coefficient (k) of the state-space formulated discrete linear cascade model (DLCM) to the concurrent discharge rate of the Tisza. As a result, the root mean square error of the 1-day forecasts decreased from $25 \text{ m}^3 \cdot \text{s}^{-1}$ ($k = 1.7 \text{ days}^{-1}$ and the number of storage elements is 2) with the corresponding Nash-Sutcliffe-type performance value of 0.95 to $11 \text{ m}^3 \cdot \text{s}^{-1}$ in the calibration period and to $15 \text{ m}^3 \cdot \text{s}^{-1}$ in the validation period (the corresponding Nash-Sutcliffe-type performance values are 0.99 and 0.98, respectively). During floods of the Tisza, the k value decreased to as little as 0.35 days^{-1} , indicating a significant slowdown of the tributary flood-wave because of the resulting backwater effect. Subsequent stage-forecasts were aided by a coupled autoregressive moving-average (1,1) model of the DLCM error sequence and the application of the Jones formula in addition to a conveyance curve, the latter yielding the most accurate 1-day forecasts with a root mean square error of 28 cm and Nash-Sutcliffe-type performance value of 0.99 for the combined (validation and calibration) time periods. The method requires no significant change in the mathematical structure of the original DLCM and thus is well-posed for inclusion of existing operational streamflow-forecasting schemes. DOI: 10.1061/(ASCE)HE.1943-5584.0000771. © 2014 American Society of Civil Engineers.

Author keywords: Flood routing; Streamflow; Rivers; Unsteady flow.

Introduction

Almost every textbook of hydrology (e.g., Beven et al. 2009) mentions that traditional flow-routing methods, because of their inherent assumptions, are not recommended for river reaches significantly affected by backwater effects. Yet, traditional flow-routing methods are still widely used in hydrological forecasting centers such as the National Hydrological Forecasting Service (NHFS) in Hungary because of the minimal data-requirement of the flow-routing methods (typically only inflow) and their very fast numerical (or analytical) solutions. One would think that such considerations would not matter in the 21st century of fast computers, but they become a factor when one deals with several hundreds of gauging stations and performs operational forecasts $2 \times$ /day (7 days/week) from 12 h up to 6 days in advance, and all that with minimal human and financial resources such as the practice at NHFS.

The discrete linear cascade model (DLCM; e.g., Szollosi-Nagy 1982) in use at NHFS is a spatially (using a backward difference scheme) and temporally discretized form of the linear kinematic wave equation (Lighthill and Witham 1955) written in a state-space form; see Szilagyi and Szollosi-Nagy (2010), Theorem 3,

p. 34. Because of the finite spatial differences involved, DLCM also approximates the diffusion wave equation (Szilagyi and Szollosi-Nagy 2010, p. 59) in its flow-routing either in a pulsed [i.e., the last measured upstream discharge rate (q_{in}) held constant in time, as piece-wise continuous input to the river reach, until the next measurement arrives (Szollosi-Nagy 1982)] or linearly interpolated (between consecutive inflow measurements) data-framework (Szilagyi 2003). In this context, the latter approach is summarized next. For a rigorous mathematical treatment on the theory, see Szilagyi and Szollosi-Nagy (2010). Over the past decade DLCM has also been applied to account for and infer stream-aquifer interactions (Szilagyi 2004; Szilagyi et al. 2006) and to detect historical changes in channel properties (Szilagyi et al. 2008).

The state and output equations of the DLCM for a river reach comprised of n number of subreaches can be written as

$$\dot{\mathbf{S}}(t) = \mathbf{F}\mathbf{S}(t) + \mathbf{G}q_{in}(t) \quad (1a)$$

$$q_{out}(t) = \mathbf{H}\mathbf{S}(t) \quad (1b)$$

where q_{out} = outflow of the stream reach; the dot denotes the time-rate of change; t = time-reference, \mathbf{F} and \mathbf{S} are the $n \times n$ state matrix and $n \times 1$ state variable, respectively; and \mathbf{G} and \mathbf{H} are the $n \times 1$ input and $1 \times n$ output vectors, defined as

$$\mathbf{F} = \begin{bmatrix} -k & & & & & \\ k & -k & & & & \\ & & \ddots & & & \\ & & & \ddots & & \\ & & & & k & -k \end{bmatrix} \quad (2a)$$

$$\mathbf{S}(t) = \begin{bmatrix} S_1(t) \\ S_2(t) \\ \vdots \\ S_n(t) \end{bmatrix} \quad (2b)$$

¹Professor, Dept. of Hydraulic and Water Resources Engineering, Budapest Univ. of Technology and Economics, H-1111 Muegyetem Rakpart 1-3, Budapest, Hungary; and School of Natural Resources, Univ. of Nebraska-Lincoln, 3310 Holdrege St., Lincoln, NE 68583 (corresponding author). E-mail: jszilagy1@unl.edu

²Junior Researcher, Dept. of Flood-Protection, Koros-Valley Water Authority, H-5700 Varoshaz utca 27, Gyula, Hungary. E-mail: laurinyecz.pal@hotmail.com

Note. This manuscript was submitted on January 18, 2012; approved on December 16, 2012; published online on December 18, 2012. Discussion period open until June 1, 2014; separate discussions must be submitted for individual papers. This paper is part of the *Journal of Hydrologic Engineering*, Vol. 19, No. 1, January 1, 2014. © ASCE, ISSN 1084-0699/2014/1-69-77/\$25.00.

$$\mathbf{G} = \begin{bmatrix} 1 \\ 0 \\ \vdots \\ 0 \end{bmatrix} \quad (2c)$$

$$\mathbf{H} = [0 \quad 0 \quad \dots \quad k] \quad (2d)$$

where S_i denotes the stored water volume in subreach i ; and k = storage coefficient of the subreach, the same value for each. The one-step-ahead (from t to $t + \Delta t$) solution of Eq. (1) in a linearly interpolated data framework becomes (Szilagyi 2003)

$$\mathbf{S}(t + \Delta t) = \mathbf{\Phi}(\Delta t)\mathbf{S}(t) + \mathbf{\Gamma}_1(\Delta t)q_{in}(t) + \mathbf{\Gamma}_2(\Delta t)q_{in}(t + \Delta t) \quad (3)$$

where $\mathbf{\Phi}$ is the corresponding $n \times n$ state-transition matrix; and $\mathbf{\Gamma}_1$ and $\mathbf{\Gamma}_2$ are the $n \times 1$ input-transition vectors, defined as

$$\mathbf{\Phi}(\Delta t) = \begin{bmatrix} e^{-k\Delta t} & & & & \\ k\Delta t e^{-k\Delta t} & e^{-k\Delta t} & & & \\ \vdots & & \ddots & & \\ \frac{(k\Delta t)^{n-1}}{(n-1)!} e^{-k\Delta t} & \frac{(k\Delta t)^{n-2}}{(n-2)!} e^{-k\Delta t} & \dots & e^{-k\Delta t} & \end{bmatrix} \quad (4a)$$

$$\mathbf{\Gamma}_1(\Delta t) = \begin{bmatrix} \frac{\Gamma(1, k\Delta t)}{k\Gamma(1)} \left[\frac{1}{k\Delta t} - \frac{e^{-k\Delta t}}{\Gamma(1, k\Delta t)} \right] \\ \frac{\Gamma(2, k\Delta t)}{k\Gamma(2)} \left[\frac{2}{k\Delta t} - \frac{k\Delta t e^{-k\Delta t}}{\Gamma(2, k\Delta t)} \right] \\ \vdots \\ \frac{\Gamma(n, k\Delta t)}{k\Gamma(n)} \left[\frac{n}{k\Delta t} - \frac{(k\Delta t)^{n-1} e^{-k\Delta t}}{\Gamma(n, k\Delta t)} \right] \end{bmatrix} \quad (4b)$$

$$\mathbf{\Gamma}_2(\Delta t) = \begin{bmatrix} \frac{\Gamma(1, k\Delta t)}{k\Gamma(1)} \left[1 - \frac{1}{k\Delta t} + \frac{e^{-k\Delta t}}{\Gamma(1, k\Delta t)} \right] \\ \frac{\Gamma(2, k\Delta t)}{k\Gamma(2)} \left[1 - \frac{2}{k\Delta t} + \frac{k\Delta t e^{-k\Delta t}}{\Gamma(2, k\Delta t)} \right] \\ \vdots \\ \frac{\Gamma(n, k\Delta t)}{k\Gamma(n)} \left[1 - \frac{n}{k\Delta t} + \frac{(k\Delta t)^{n-1} e^{-k\Delta t}}{\Gamma(n, k\Delta t)} \right] \end{bmatrix} \quad (4c)$$

where $\Gamma(\cdot)$ with one argument are the complete gamma functions, and with two arguments are the incomplete gamma functions, as defined by Abramowitz and Stegun (1965). During actual forecasting the inflow at $t + \Delta t$ is not yet known but is estimated from another streamflow-routing upstream. The streamflow forecast is obtained by applying the output [Eq. (1)] over Eq. (3), which is the multiplication of S_n at $t + \Delta t$ by k . The linearly interpolated data framework for flow-routing is expected to yield more accurate forecasts than the classical pulsed-data framework because it represents streamflow more realistically than the latter (which assumes sudden jumps in the flow value at the time of the measurements).

The state-space formulation allows for a simple estimation of the initial condition (Szilagyi and Szollosi-Nagy 2010), which is the distribution of the stored water volumes in each subreach at the start of predictions, eliminating the need of starting the calculations from a relaxed state or from a near steady-state, as is the requirement of classical linear flow-routing techniques.

The model has two parameters to calibrate, (1) the number of sub-reaches n , and (2) the storage coefficient k of each subreach. If the length (L) of the river reach is known, then calibration is helped by the fact that Lkn^{-1} yields the mean flood-wave celerity (the value of which can be fairly well estimated within a narrow range from records of concurrent upstream and downstream flow

rates), which significantly restricts the possible choices for the k and n value combinations, thus speeding up considerably any trial-and-error calibration, for example. For river reaches with notable backwater effects (e.g., tidal rivers or tributary junctions) and/or floodplains, the wave celerity may change with respect to time, necessitating modification of the original model or its output by different adjustment methods. For example, river reaches with floodplains are often modeled through an amplitude distribution scheme, in which the inflow rate is deconstructed into several components depending on how the inflow value falls into predefined intervals (Becker and Kundzewicz 1987). Each inflow component is then routed separately by linear models having differing parameters and the results summed. This so-called multilinear flow-routing approach [including also a time distribution scheme of the inflows; e.g., Perumal et al. (2009)] does not account for backwater effects, as Becker and Kundzewicz (1987) noted. A simple method is discussed next that addresses how to account for backwater effects in the DLCM.

Accounting for Backwater Effects in the DLCM

The one-step-ahead solution of Eq. (3) calculates the distribution of subreach storages for $t + \Delta t$ in each time t , with the actual storage coefficient k . For example, at tributary confluences, the primary-stem river stage/discharge often influences the dynamics of the flood-wave propagation along the tributary near the junction by slowing it down during simultaneous flood conditions on the primary stem. This way, the storage coefficient value k can be conditioned on the concurrent primary-stem discharge/stage value, leading to temporally changing $k(t)$ values that remain constant with respect to each computational time interval Δt in Eq. (3). In the study area in Hungary (Figs. 1 and 2), the confluence of the Tisza (mean annual flow Q_m of $550 \text{ m}^3 \cdot \text{s}^{-1}$ at Csongrad) and its tributary, the Koros River ($Q_m = 105 \text{ m}^3 \cdot \text{s}^{-1}$ at Kunszentmarton), such a relationship was sought.

Flow-routing on the Koros River took place between Gyoma and Kunszentmarton, a 58-km river stretch (the channel-bottom slope S_0 is $4 \text{ cm} \cdot \text{km}^{-1}$), which takes in the unmeasured flow of the Hortobagy-Berettyo drainage and irrigation canal (Fig. 2). To account for this unknown quantity of water, the Hydraulic Engineering Centers River Analysis System (HEC-RAS; USACE 2010) one-dimensional (1-D) hydraulic model was employed for the Tisza by staff of the Middle-Tisza Water Authority, between Szolnok [with measured flow-rate as upper boundary condition (BC)] and Mindszent (with measured stage as lower BC), and simultaneously for the Koros between Gyoma (measured flow-rate BC) and Csongrad to obtain the flow rates at Kunszentmarton, without the contribution of the Hortobagy-Berettyo Canal for the October 1, 2010–September 30, 2011, time period. The HEC-RAS model had previously been calibrated with detailed cross-sectional data on both rivers for the 2006 flood period on the Tisza. Fig. 3 displays the HEC-RAS model results when the measured streamflow rates at Gyoma were augmented by the difference in the measured and HEC-RAS-obtained values at Kunszentmarton by adding this difference to the measured flow at Gyoma before executing HEC-RAS again. For evaluation of the DLCM, this corrected HEC-RAS-obtained time-series is used (in place of the measured values at Kunszentmarton) subsequently to separate the effect of the unknown flow-rates of the Hortobagy-Berettyo canal on the performance of DLCM.

Employing a trial-and-error method (in a root mean square sense) and $\Delta t = 1$ day, DLCM calibration (for February 1, 2011–September 30, 2011) yielded $n = 2$ and $k = 1.7 \text{ days}^{-1}$



Fig. 1. Location of the study area within Hungary

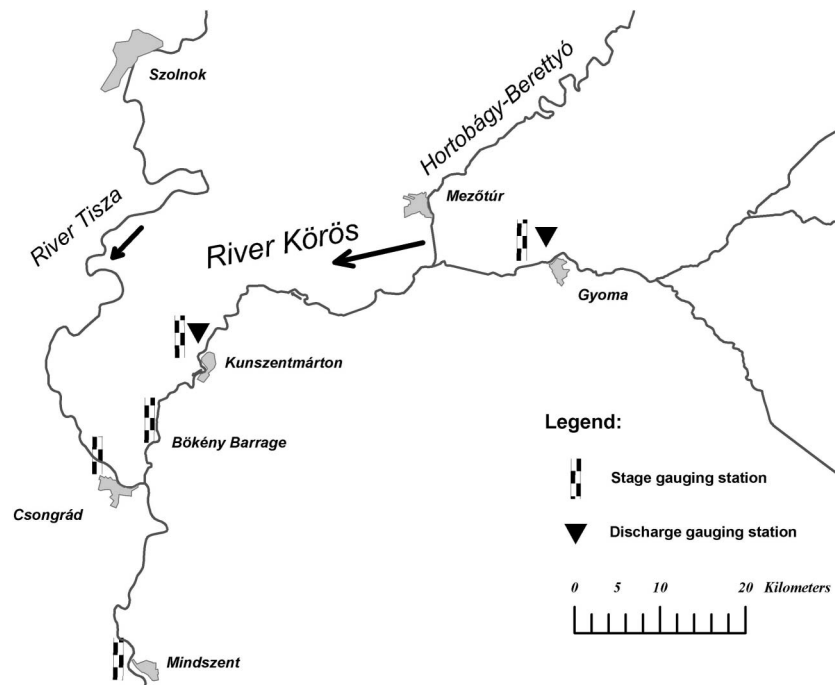


Fig. 2. Confluence of the Tisza and Koros Rivers

with root mean square error (RMSE) = $25 \text{ m}^3 \cdot \text{s}^{-1}$ and Nash-Sutcliffe-type (NSC) performance value = $1 - (\text{RMSE}/\text{SD})^2 = 0.95$ (where SD = standard deviation of the daily discharge values) for the October 1, 2010–September 30, 2011, time period. The established calibration period is shorter than the original data record because the extended flood-event on the Tisza (Fig. 4) and its backwater effect on the Koros were intended to be excluded from the calibration to have a model that works truly optimally during backwater-free periods. Fig. 4 displays the results of the flow-routing. As long as the flow rate of the Tisza is less than about $600 \text{ m}^3 \cdot \text{s}^{-1}$, the DLCM is fairly accurate, but in time periods when the Tisza has a flood, the DLCM responds too fast on both the rising and falling limbs of the flood wave. Rather than

conditioning the storage coefficient value k on the discharge of the Tisza, its inverse $K = k^{-1}$ is used; because K yields the average residence time of the flood wave within the subreach and with increasing flow rate of the Tisza, this residence time would also be expected to increase. As a result, K was related to the discharge rate of the Tisza at Csongrad (Q_T , obtained from HEC-RAS) in excess of a threshold value $Q_{th} = 600 \text{ m}^3 \cdot \text{s}^{-1}$

$$K(t) = a[Q_T(t) - Q_{th}]^b + K \quad (5)$$

where a and b are constants to be calibrated; and $K = k^{-1} = 1.7^{-1} = 0.59 \text{ days} = 50,976 \text{ s}$. Trial-and-error optimization (again in a root mean square sense) yielded $a = 146.88 \text{ s}^2 \cdot \text{m}^{-3}$

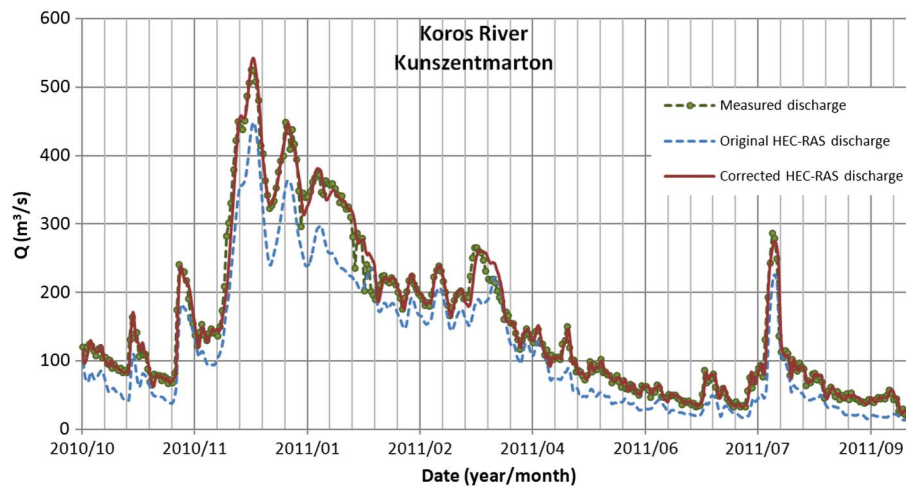


Fig. 3. Reconstructed streamflow time-series of the Koros River at Kunszentmarton by HEC-RAS, accounting for the unknown flow rates of the Hortobagy-Berettyo canal; original discharge indicates HEC-RAS-modeled values from measured discharge at Gyoma; corrected indicates HEC-RAS-modeled values from measured discharge at Gyoma augmented by the difference (measured and original HEC-RAS-modeled) at Kunszentmarton

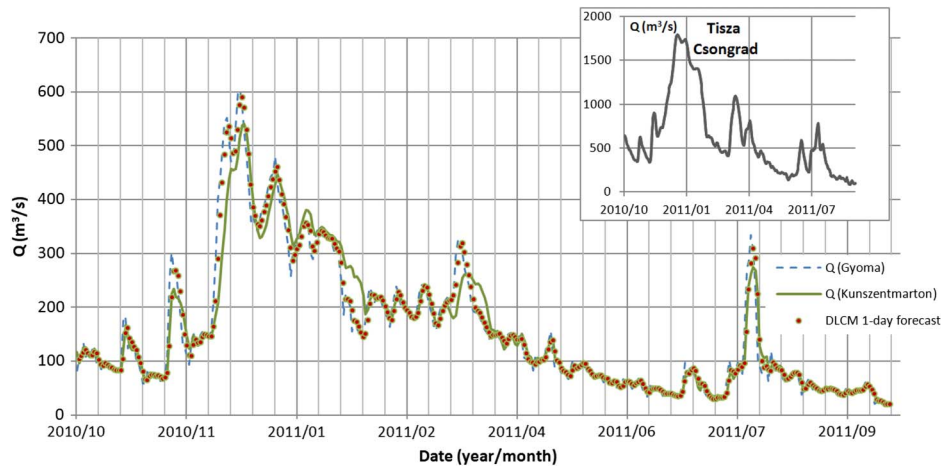


Fig. 4. Discrete linear cascade model flow-routing results ($n = 2$, $\Delta t = 1$ day) with a constant storage coefficient ($k = 1.7 \text{ day}^{-1}$), October 1, 2010–September 30, 2011; Q (Kunszentmarton) denotes the corrected HEC-RAS-obtained flow values; the inset displays the concurrent discharge of the Tisza at Csongrad

and $b = 1$. Fig. 5 depicts the dependence of the $K(t)$ and $k(t)$ values on the flow rate of the Tisza at Csongrad. Similar investigation was done with stage values (employing meters at an elevation greater than mean sea level) in place of the discharge rates in Eq. (5) with a threshold value of 80 m (corresponding with $Q_{th} = 600 \text{ m}^3 \cdot \text{s}^{-1}$), but it yielded a nonlinear relationship ($b = 0.8$) and a somewhat worse performance than the discharge values. The obtained values of the parameters (a , b) in Eq. (5), in addition to the critical discharge value, are site-specific, changing by location. However, the approach of relating the value of K to some measure of the extent of the composite backwater effect is expected to be transferable in general.

Application of a time-varying storage coefficient by Eq. (5) brought a significant improvement in the DLCM predictions (Fig. 6), with $\text{RMSE} = 11 \text{ m}^3 \cdot \text{s}^{-1}$ (44% of the original value) and $\text{NSC} = 0.99$. Fig. 7 displays the resulting change in the storage coefficient and the kinematic-wave celerity values,

$c(t) = Lk(t)n^{-1}$. The flood waves of the Koros River slow down considerably (from about $2 \text{ km} \cdot \text{h}^{-1}$ to less than $0.5 \text{ km} \cdot \text{h}^{-1}$) during backwater effects, leading to a flattening and spreading out of the flood wave. Validation of the method was performed on a 2-year period (October 1, 2008–September 30, 2010) preceding the calibration period and yielded $\text{RMSE} = 15 \text{ m}^3 \cdot \text{s}^{-1}$ and $\text{NSC} = 0.98$, which are slightly worse than the calibration results. When the validation and calibration periods are combined, the model has $\text{RMSE} = 14 \text{ m}^3 \cdot \text{s}^{-1}$ and $\text{NSC} = 0.984$.

Stochastic Submodel of DLCM Prediction Errors

As is the case with most deterministic flow-routing models, the prediction error sequence displays a high degree of autocorrelation [Fig. 8(a)]. As the simplest solution to improve model performance, deterministic models are often combined with an additional stochastic submodel (Szilagyi and Szollosi-Nagy 2010). The writers

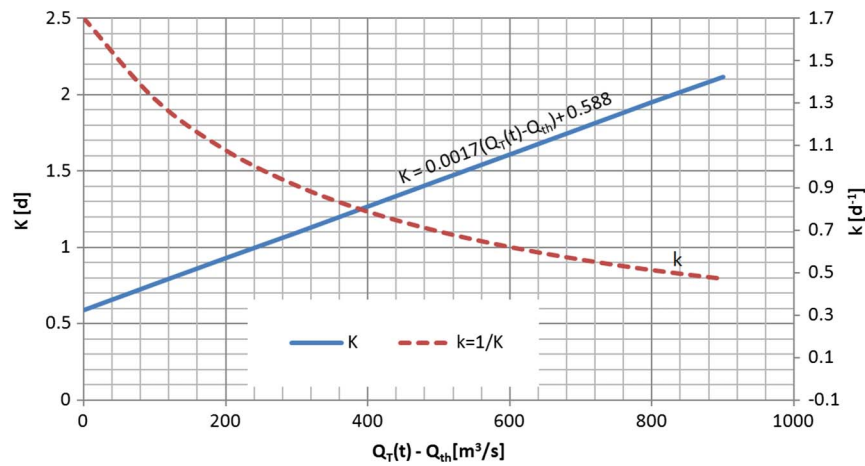


Fig. 5. Dependence of the mean residence time $K(t)$ and storage coefficient $k(t)$ values on the flow rate of the Tisza at Csongrad (Q_T) greater than a threshold value of $Q_{th} = 600 \text{ m}^3 \cdot \text{s}^{-1}$; in the equation for K the flow rates must be defined in $\text{m}^3 \cdot \text{day}^{-1}$

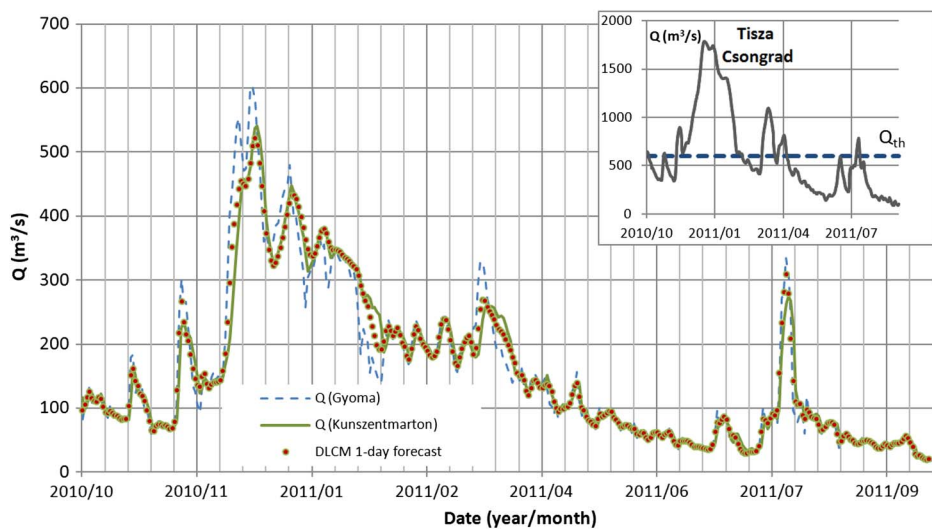


Fig. 6. Discrete linear cascade model flow-routing results ($n = 2$, $\Delta t = 1$ day) with a time-varying storage coefficient (a function of the Tisza River flow rate at Csongrad), calibration period of October 1, 2010–September 30, 2011; Q (Kunszentmarton) denotes the corrected HEC-RAS-obtained flow values; the inset displays the concurrent discharge of the Tisza at Csongrad

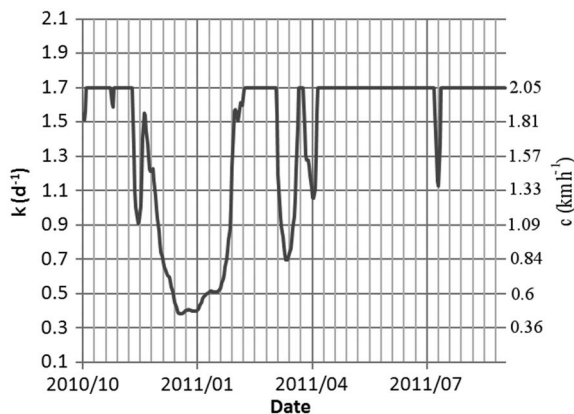


Fig. 7. Temporal change in the storage coefficient $k(t)$ and flood-wave celerity $c(t)$ values in the calibration period, October 1, 2010–September 30, 2011

tried the simplest first-order and second-order autoregressive [AR(1), AR(2)] in addition to autoregressive moving average [ARMA(1,1)] models, and found the latter the best-performing. Defining model error as the predicted value minus the observed value, the coupled deterministic-stochastic model's one-step-ahead prediction (i.e., the conditional expectation with the condition of having the values observed at time t) will become

$$\hat{Q}^*(t + \Delta t) = \mathbf{HS}(t + \Delta t) - \Phi[\hat{Q}(t) - Q(t)] + \theta[\hat{Q}(t) - \hat{Q}^*(t)] \quad (6)$$

where $\hat{Q} =$ DLCM 1-day prediction of the flow rate (Q) at Kunszentmarton; and $\hat{Q}^* =$ combined DLCM-ARMA(1,1) 1-day prediction of the flow rate (Q) at Kunszentmarton. The estimated values of $\varphi = 0.68$ and $\theta = -0.72$ for the autoregressive and moving-average coefficients, respectively, came from the method of moments equations; e.g., Box et al. (1994)

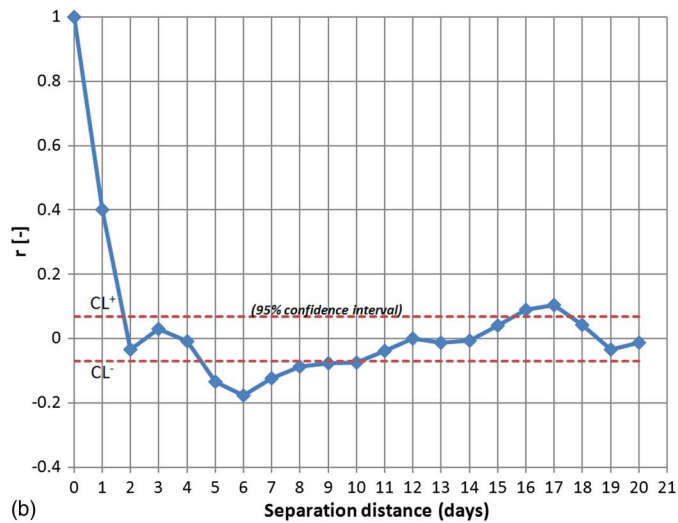
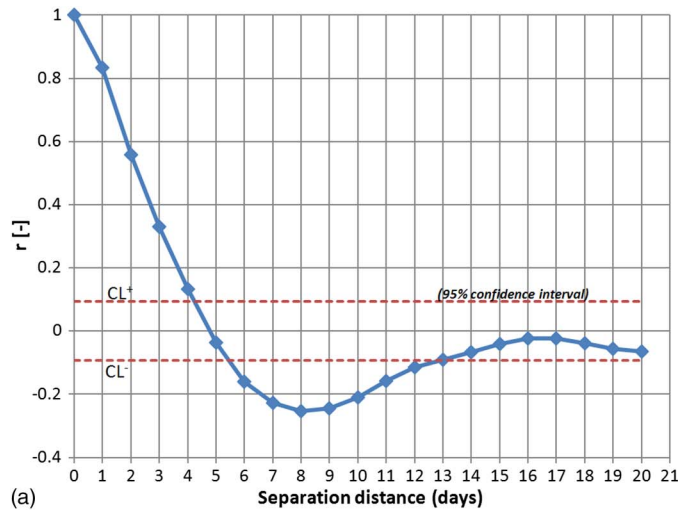


Fig. 8. Autocorrelation function with respect to the calibration period of October 1, 2010–September 30, 2011: (a) DLCM; (b) DLCM-ARMA(1,1) model errors

$$r_1 = \frac{(1 - \varphi\theta)(\varphi - \theta)}{1 + \theta^2 - 2\varphi\theta} \quad (7a)$$

$$r_2 = \varphi r_1 \quad (7b)$$

where r_1 and r_2 = one-step and two-step sample autocorrelation coefficient values [Fig. 8(a)] of the DLCM errors. Fig. 8(b) displays the autocorrelation function of model errors for the combined deterministic-stochastic model. Although the chosen stochastic model is not perfect (several values fall outside the confidence interval), it has the distinct advantage of being simple, and having only two parameters the optimized values are expected to be relatively stable. Compared with the original DLCM, the RMSE decreased from 11 to 9 $\text{m}^3 \cdot \text{s}^{-1}$, whereas the NSC value improved in the third decimal (from 0.991 to 0.994). At very large values of NSC, the value changes relatively little to even significant improvements in the RMSE value (about a 20% decrease); Fig. 9 shows the combined model results.

Stage Forecasting with the Combined DLCM-ARMA (1,1) Model

In flood-defense practice the primary information is stage level instead of the discharge rate. Even an accurate flow-routing model in discharge values may be inaccurate in stage values without the correct transformation of the discharge rates into stage levels (Fig. 10). This inaccuracy is not surprising after evaluating the permanent rating curve and the HEC-RAS-derived concurrent discharge Q and stage H values (Fig. 11), indicating a significant loop in the Q versus H relationship at Kunszentmarton.

To account for the loop-rating curve, first the Jones formula was applied (Fenton 2001)

$$Q(t) = Q_0(t) \sqrt{1 + \frac{1}{S_0 c(t)} \frac{\partial H(t)}{\partial t} - \frac{D(t)}{c^3(t)} \frac{\partial^2 H(t)}{\partial t^2}} \quad (8)$$

where Q_0 = permanent discharge value; and D = diffusion coefficient = $Q(2BS_0)^{-1}$, where B = channel width. The diffusion term contributes very little to the outcome and it was subsequently

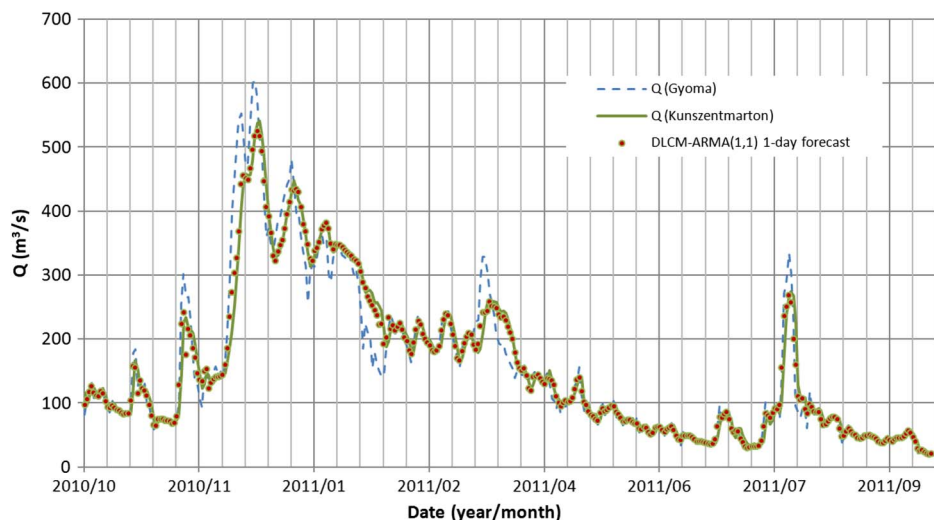


Fig. 9. Combined deterministic-stochastic DLCM-ARMA(1,1) flow-routing results ($n = 2$, $\Delta t = 1$ day) with a time-varying storage coefficient (a function of the Tisza River flowrate at Csongrad), calibration period of October 1, 2010–September 30, 2011; Q (Kunszentmarton) denotes the corrected HEC-RAS-obtained flow values

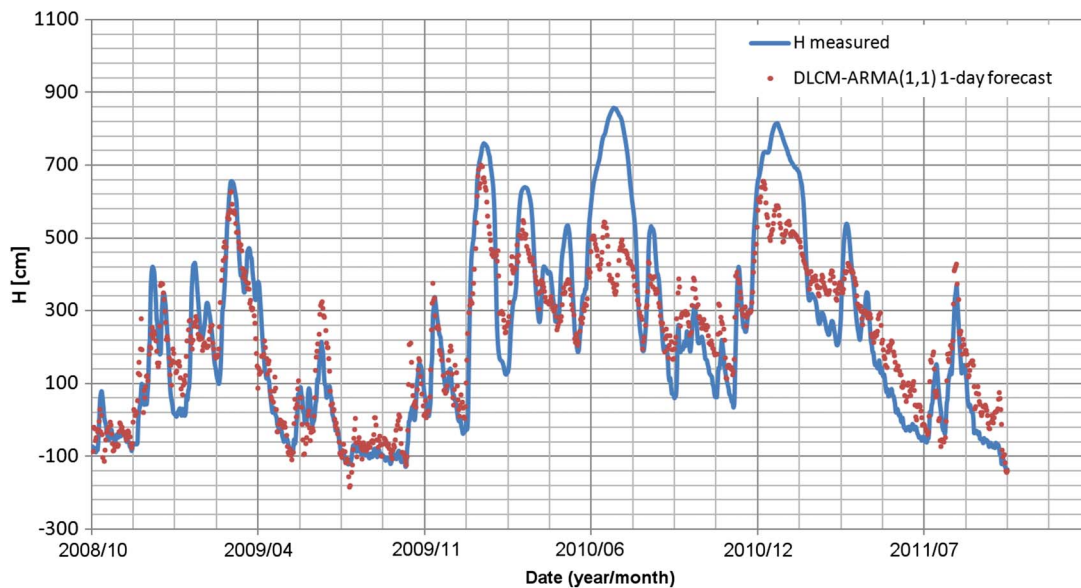


Fig. 10. Measured and DLCM-ARMA(1,1)-predicted stage levels at Kunszentmarton with the help of a permanent rating curve (October 1, 2008–September 30, 2011); RMSE = 118 cm and NSC = 0.24

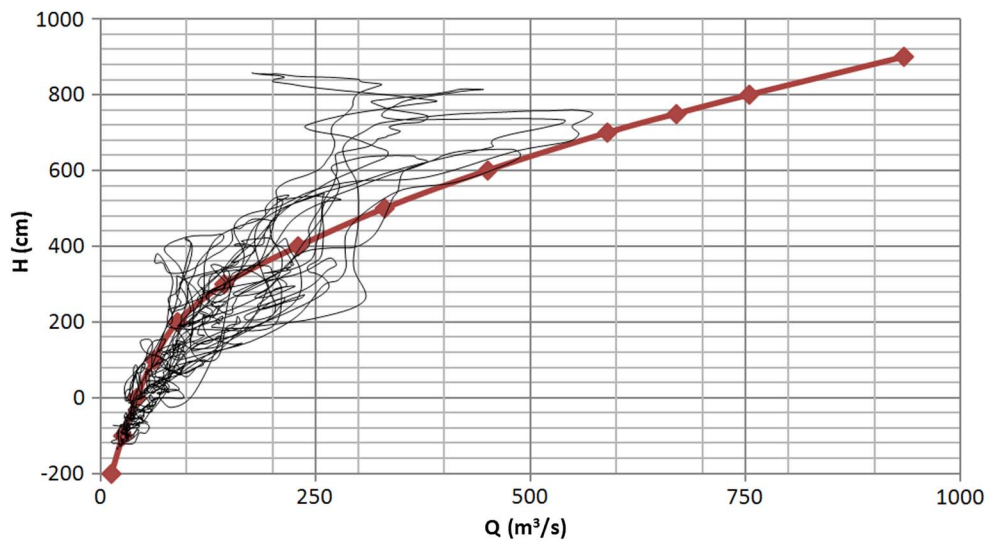


Fig. 11. Permanent rating curve for Kunszentmarton and the concurrent Q versus H values derived from HEC-RAS

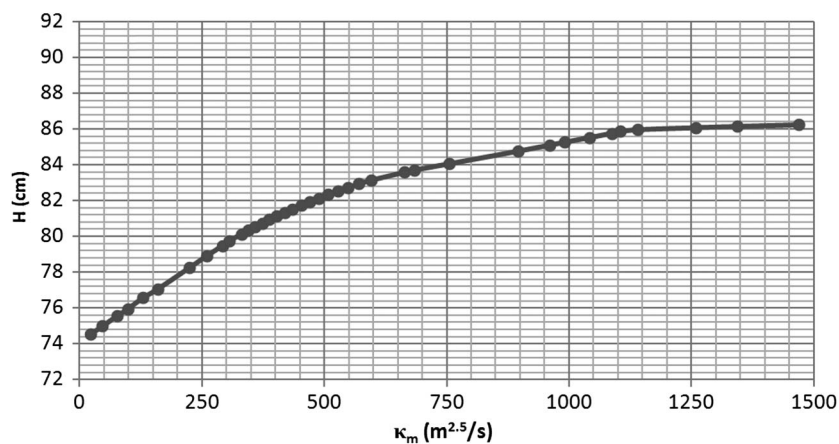


Fig. 12. Modified conveyance curve for Kunszentmarton

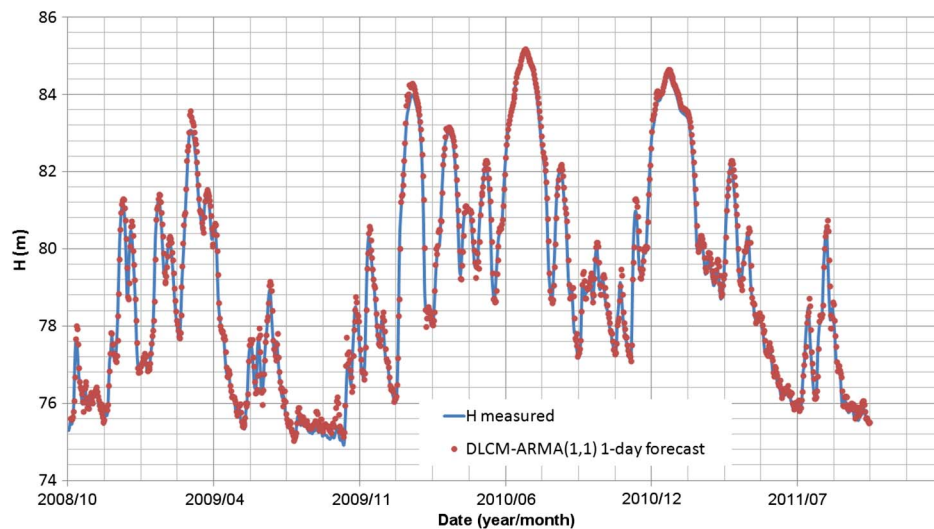


Fig. 13. Measured and DLCM-ARMA(1,1)-predicted stage levels at Kunszentmarton with the help of the modified conveyance curve (October 1, 2008–September 30, 2011); RMSE = 28 cm and NSC = 0.99

Table 1. Root Mean Square Error and Nash-Sutcliffe-Type Performance Values for Different Model Setups

RMSE, $\text{m}^3 \cdot \text{s}^{-1}$ for Q and cm for h , and NSC (%) values	DLCM with constant $k = 1.7 \text{ days}^{-1}$	DLCM with time-varying $k, k(t)$	DLCM-ARMA (1,1) with $k(t)$	DLCM-ARMA(1,1) with $k(t)$, permanent rating curve	DLCM-ARMA(1,1) with $k(t)$, conveyance function
Predicted variable	Q	Q	Q	h	h
Calibration period, October 2010–September 2011	25, 95; calibration period February–September 2011	11, 99.1	9, 99.4	113, 31	24, 99.5
Verification period, October 2008–September 2010	33, 91	15, 98	11, 98.9	134, 17	30, 99.2
Combined period, October 2008–September 2011	30, 92	14.25, 98.4	10.38, 99.1	118, 24	28, 99.3

Note: h = stage value (at Kunszentmarton); k = storage coefficient of DLCM; and Q = discharge (at Kunszentmarton).

neglected in the Q to H transformations. Eq. (8) is implicit in the desired H value. Application of the Jones formula improved the stage forecast only moderately, by a 17% decrease in RMSE; consequently, an alternative solution, the application of the conveyance function κ , was selected in the form (Fenton 2001)

$$Q(t) = \kappa[H(t)]\sqrt{S_H(t)} \approx \kappa_m[H(t)]\sqrt{H_{KM}(t) - H_B(t)} \quad (9)$$

where S_H = slope of the streamwater surface; $\kappa_m = \kappa L^{-1/2}$, which is the modified conveyance function (Fig. 12) derived by the staff of the Koros-Valley Water Authority; and H_{KM} and H_B = stage levels at Kunszentmarton and Bokeny (Fig. 2), respectively. Eq. (9) is a bivariate rating curve. Rearrangement of Eq. (9) yields the DLCM-ARMA(1,1) 1-day forecast of the stage at Kunszentmarton

$$\hat{H}_{KM}^*(t + \Delta t) = \left[\frac{\hat{Q}_{KM}^*(t + \Delta t)}{\kappa_m(t)} \right]^2 + \hat{H}_B(t + \Delta t) \quad (10)$$

where the predicted stage level at Bokeny (\hat{H}_B) is obtained by a backward difference-scheme as $\hat{H}_B(t + \Delta t) = 2H_B(t) - H_B(t - \Delta t)$. Fig. 13 displays the resulting 1-day stage forecasts. Compared with the forecasts using a permanent rating curve, the RMSE value changed from 118–28 cm, and the corresponding NSC value from 0.24–0.99, a significant improvement in both measures. The stage forecasts became as efficient in accuracy as the discharge forecasts (Table 1).

Summary and Conclusions

The DLCM is a physically based flow-routing method (Szollosi-Nagy 1982) written in a state-space form that explicitly accounts for the temporally and spatially discrete nature of the input data. It has two parameters, (1) the number of subreaches, and (2) their storage coefficient.

The significant backwater effect of the Tisza on its tributary, the Koros River, was accounted by relating the value of the storage coefficient k to the flow rate of the Tisza. The value of k thus changes between each routing time-step, which was chosen to be 1 day. The changing value of k does not cause any additional difficulties in a state-space form as long as the multiple-step predictions are done recursively [i.e., by the repetitive application of Eq. (3) with an update of the storage coefficient value in each time step] and not through an explicit discrete convolution.

The deterministic flow-routing of DLCM was also augmented by an additional stochastic ARMA (1,1) model component. Because in flood-defense practice, stage forecasts are more valuable than forecasted discharges, the latter were transformed into stage values by application of a permanent rating curve. Given the large inaccuracy (not least because of the significant backwater effect of the Tisza) of the stage forecasts, the Jones formula was subsequently applied with moderately improved predicted values. Thus, the Jones formula was replaced by a conveyance function, which implies a bivariate rating curve in which flow rate is not

only determined by stage but also by the slope of the water surface. This way, the accuracy of the discharge forecasts were recaptured in the ensuing stage forecasts with NSC = 0.99.

The described method is the first such application of the DLCM (i.e., accounting for backwater effects by changing the storage coefficient value of the cascade) to the writers' best knowledge. The method does not require any hydraulic parameter of the stream reach in which routing takes place. If the length of the reach is known, it helps speed up the parameter-calibration process. In this paper, the k values were related to the discharge rate of the Tisza but in other applications the employment of stage values may yield better results. The suggested adjustment of the storage coefficient can also be achieved in amplitude distribution multilinear model situations (Becker and Kundzewicz 1987), in which, for example, two cascades are set up in parallel, describing (1) channel flow, and (2) floodplain flow conditions. Adjustment of the k values (two in this manner) may then happen separately.

Acknowledgments

This paper was supported by the Hungarian Scientific Research Fund (OTKA, no. 83376) and the Agricultural Research Division of the University of Nebraska. This paper is connected to the scientific program of the Development of Quality-Oriented and Harmonized R + D + I Strategy and Functional Model at BME project. This project is supported by the New Szechenyi Plan (project ID TAMOP-4.2.1/B-09/1/KMR-2010-0002). The writers thank the anonymous reviewers for their valuable comments on a previous version of the paper.

Notation

The following symbols are used in this paper:

- a = empirical coefficient ($L^{-3} \cdot T^2$);
- b = empirical coefficient;
- c = kinematic-wave celerity ($L \cdot T^{-1}$);
- D = diffusion coefficient ($L^2 \cdot T^{-1}$);
- \mathbf{F} = $n \times n$ state matrix;
- \mathbf{G} = $n \times 1$ input vector;
- H = stage level (L);
- \mathbf{H} = $1 \times n$ output vector (T^{-1});
- \hat{H} = predicted stage level, using a backward-difference scheme (L);
- \hat{Q}^* = 1-day-ahead DLCM-ARMA(1,1) model prediction of the stage level (L);
- K = mean residence time (T), the inverse of k ;
- k = storage coefficient (T^{-1});
- L = river-reach length (L);
- n = number of subreaches;
- Q = streamflow rate ($L^3 \cdot T^{-1}$);
- Q_m = mean annual streamflow rate ($L^3 \cdot T^{-1}$);
- Q_T = streamflow rate of the Tisza at Csongrad ($L^3 \cdot T^{-1}$);
- Q_{th} = threshold flow-rate value of the Tisza at Csongrad ($L^3 \cdot T^{-1}$);
- \hat{Q} = 1-day-ahead DLCM prediction of the discharge rate ($L^3 \cdot T^{-1}$);

- \hat{Q}^* = 1-day-ahead DLCM-ARMA(1,1) model prediction of the discharge rate ($L^3 \cdot T^{-1}$);
- q_{in} = river-reach inflow rate ($L^3 \cdot T^{-1}$);
- q_{out} = river-reach outflow rate ($L^3 \cdot T^{-1}$);
- r_1 = one-step sample autocorrelation coefficient;
- r_2 = two-step sample autocorrelation coefficient;
- \mathbf{S} = $n \times 1$ state vector (L^3);
- S_i = water storage in the i th subreach (L^3);
- S_0 = channel-bottom slope;
- t = time (T);
- $\mathbf{\Gamma}$ = $n \times 1$ input-transition vector;
- $\Gamma(\cdot)$ = complete (with one argument) or incomplete (with two arguments) gamma function;
- Δt = routing time-step (T);
- θ = moving-average coefficient;
- κ = conveyance function ($L^3 \cdot T^{-1}$);
- κ_m = modified conveyance function, $\kappa_m = \kappa L^{-1/2} (L^{2.5} \cdot T^{-1})$;
- Φ = $n \times n$ state-transition matrix; and
- φ = autoregressive coefficient.

References

- Abramowitz, M., and Stegun, I. A. (1965). *Handbook of mathematical functions*, Dover, New York.
- Becker, A., and Kundzewicz, Z. W. (1987). "Nonlinear flood routing with multilinear models." *Water Resour. Res.*, 23(6), 1043–1048.
- Beven, K., Shaw, E. M., Chappell, N. A., and Lamb, R. (2009). *Hydrology in practice*, 4th Ed., Taylor and Francis, New York.
- Box, G. E. P., Jenkins, G. M., and Reinsel, G. C. (1994). *Time series analysis, forecasting and control*, 3rd Ed., Prentice Hall, Upper Saddle River, NJ.
- Fenton, J. D. (2001). "Rating curves: Part 1—Correction for surface slope." *Proc., Conf. on Hydraulics in Civil Engineering*, Institution of Engineers, Barton, Australia, 309–317.
- Lighthill, M. J., and Witham, G. B. (1955). "On kinematic floods. I: Flood movements in long rivers." *Proc. Roy. Soc. London Ser. A Math. Phys. Sci.*, 229(1178), 281–316.
- Perumal, M., Sahoo, B., Moramarco, T., and Barbetta, S. (2009). "Multilinear Muskingum method for stage-hydrograph routing in compound channels." *J. Hydrol. Eng.*, 10.1061/(ASCE)HE.1943-5584.0000029, 663–670.
- Szilagyi, J. (2003). "State-space discretization of the KMN-cascade in a sample-data system framework for streamflow forecasting." *J. Hydrol. Eng.*, 10.1061/(ASCE)1084-0699(2003)8:6(339), 339–347.
- Szilagyi, J. (2004). "Accounting for stream-aquifer interactions in the state-space discretization of the KMN-cascade for streamflow forecasting." *J. Hydrol. Eng.*, 10.1061/(ASCE)1084-0699(2004)9:2(135), 135–143.
- Szilagyi, J., Parlange, M. B., and Balint, G. (2006). "Assessing stream-aquifer interactions through inverse modeling of flow routing." *J. Hydrol.*, 327(1), 208–218.
- Szilagyi, J., Pinter, N., and Venczel, R. (2008). "Application of a routing model for detecting channel flow changes with minimal data." *J. Hydrol. Eng.*, 10.1061/(ASCE)1084-0699(2008)13:6(521), 521–526.
- Szilagyi, J., and Szollosi-Nagy, A. (2010). *Recursive streamflow forecasting: A state-space approach*, Taylor and Francis, New York.
- Szollosi-Nagy, A. (1982). "The discretization of the continuous linear cascade by means of state-space analysis." *J. Hydrol.*, 58(3), 223–236.
- U.S. Army Corps of Engineers (USACE). (2010). "Hydraulic reference manual 4.1." (<http://www.hec.usace.army.mil/software/hec-ras>) (Sep. 27, 2013).